View metadata, citation and similar papers at core.ac.uk
brought to you by CORE
provided by RERO DOC Digital Library

Published in "The FASEB Journal 30(9): 3124–3132, 2016"
which should be cited to refer to this work.

JNK1 ablation in mice confers long-term metabolic protection from diet-induced obesity at the cost of moderate skin oxidative damage

Barbara Becattini,[*,1,2] Fabio Zani,[*,1] Ludovic Breasson,[*,2] Claudia Sardi,[*,2] Vito Giuseppe D'Agostino,[†] Min-Kyung Choo,[‡] Alessandro Provenzani,[†] Jin Mo Park,[‡] and Giovanni Solinas[*,3]

[*]Laboratory of Metabolic Stress Biology, Department of Medicine, University of Fribourg, Fribourg, Switzerland; [†]Center for Integrative Biology, University of Trento, Trento, Italy; and, [‡]Cutaneous Biology Research Center, Massachusetts General Hospital and Harvard Medical School, Charlestown, Massachusetts, USA

ABSTRACT: Obesity and insulin resistance are associated with oxidative stress, which may be implicated in the progression of obesity-related diseases. The kinase JNK1 has emerged as a promising drug target for the treatment of obesity and type 2 diabetes. JNK1 is also a key mediator of the oxidative stress response, which can promote cell death or survival, depending on the magnitude and context of its activation. In this article, we describe a study in which the long-term effects of JNK1 inactivation on glucose homeostasis and oxidative stress in obese mice were investigated for the first time. Mice lacking JNK1 (JNK1$^{-/-}$) were fed an obesogenic high-fat diet (HFD) for a long period. JNK1$^{-/-}$ mice fed an HFD for the long term had reduced expression of antioxidant genes in their skin, more skin oxidative damage, and increased epidermal thickness and inflammation compared with the effects in control wild-type mice. However, we also observed that the protection from obesity, adipose tissue inflammation, steatosis, and insulin resistance, conferred by JNK1 ablation, was sustained over a long period and was paralleled by decreased oxidative damage in fat and liver. We conclude that compounds targeting JNK1 activity in brain and adipose tissue, which do not accumulate in the skin, may be safer and most effective.—Becattini, B., Zani, F., Breasson, L., Sardi, C., D'Agostino, V. G., Choo, M.-K., Provenzani, A., Park, J. M., Solinas, G. JNK1 ablation inmice confers long-termmetabolic protection from diet-induced obesity at the cost of moderate skin oxidative damage.

KEY WORDS: type-2 diabetes · insulin resistance · metabolic inflammation · antioxidants · oxidative stress tolerance

It is now appreciated that the saturation of adipocyte lipid storage capacity, the consequent ectopic lipid deposition, metabolic inflammation, and insulin resistance are closely correlated events and hallmarks of obesity-associated diseases (1–6). JNK-1 and -2 emerged as a major link between obesity-driven lipotoxicity, metabolic inflammation, and insulin resistance (1, 2, 7, 8), with JNK1 being the most important isoform (8, 9). JNK1 is activated by saturated fatty acids, and mice lacking JNK1 have reduced adiposity, reduced metabolic inflammation, and improved insulin sensitivity (8, 10, 11). JNK1 was initially believed to promote insulin resistance by direct phosphorylation of the insulin receptor substrates (7, 8, 10, 12). However, current evidence indicates that part of the improved insulin sensitivity in mice lacking JNK1 is an indirect consequence of their leaner phenotype (11, 13), which depends on JNK1 activity in neurons (13–15). Moreover, JNK1 activity in myeloid cells plays an important role in the development of obesity-driven metabolic inflammation, which further promotes insulin resistance (11, 16, 17).

Although current studies consistently indicate that JNK1 is a promising drug target for the treatment of obesity-driven insulin resistance, the long-term efficacy of JNK1 ablation for the treatment of obesity-related diseases is unknown, and there are safety concerns. Obesity and diabetes are conditions associated with oxidative stress (18, 19), and JNK1 is a central mediator of the physiologic response to oxidative stress, with outcomes ranging from increased survival to cell death, depending on intensity, length, and context of its activation (20–22). JNK was shown to promote tolerance to oxidative stress and

ABBREVIATIONS: CLS, crown-like structure; GTT, glucose tolerance; HFD, high-fat diet; HO, heme oxygenase; ITT, insulin tolerance; MDA, malondialdehyde; qPCR, quantitative PCR; Sesn, sestrin; SOD, superoxide dismutase; WT, wild-type

[1] These authors contributed equally to this work.
[2] Current affiliation: The Wallenberg Laboratory, Department of Molecular and Clinical Medicine, University of Gothenburg, Gothenburg, Sweden.
[3] Correspondence: The Wallenberg Laboratory, Department of Molecular and Clinical Medicine, University of Gothenburg, 41345 Gothenburg, Sweden. E-mail: giovanni.solinas@wlab.gu.se

increase life span in *Drosophila* and in *Caenorhabditis elegans*, by a mechanism involving increased Forkhead box O (FoxO)-dependent antioxidant defense (23–26). JNK is a major signal transducer mediating FoxO activation in response to oxidative stress (20, 27), and controls the expression of the antioxidant proteins sestrin-2 (Sesn2) and heme oxygenase (HO)-1 *via* the transcription factor AP-1 (28–31). Mouse embryonic fibroblasts lacking JNK1 and -2 display increased sensitivity to hydrogen peroxide, indicating that JNK activity sustains oxidative stress tolerance in vertebrate cells (32). Finally, the well-documented action of sustained JNK activation in promoting apoptosis in response to oxidative stress may also play an important role in tissue homeostasis by eliminating irreversibly damaged cells, hence preventing the excessive inflammation that would result from a necrotic cell (20–22). However, the physiologic and pathophysiological relevance of JNK1-induced oxidative stress tolerance in vertebrates, in particular in mouse models of obesity and insulin resistance, is unknown. Indeed, whereas JNK1 inactivation is known to protect mice from diet-induced obesity, metabolic inflammation, and insulin resistance, it must be noted that current studies are limited to 20-wk exposure to a high-fat diet (HFD) (11). Hence, the long-term effects of JNK1 inactivation in obesity are unknown. To learn about the safety and efficacy of long-term JNK1 inactivation for the treatment of obesity-driven insulin resistance, we investigated metabolic homeostasis and oxidative stress in mice lacking JNK1 ($JNK1^{-/-}$) fed an obesogenic HFD for a long period. Our results indicate that systemic inactivation of JNK1 leads to prolonged metabolic protection from diet-induced obesity and reduced oxidative damage in liver and adipose tissue, at the cost of increased predisposition to skin oxidative damage.

MATERIALS AND METHODS

In vivo studies

Mice were males on a pure C57BL6/J background, and $JNK1^{-/-}$ mice were bred as previously described (11). An HFD (60% of calories from fat) was purchased from Bio-Serv (diet F3282; Flemington, NJ, USA). The mice were kept at our standard facility in a 12 h light–dark cycle at room temperature (23°C). Two independent cohorts from different breeders were investigated. For the first cohort 15 wild-type (WT) mice and 15 $JNK1^{-/-}$ mice were weaned onto an HFD and maintained on it. For the second cohort, 9 WT mice and 12 $JNK1^{-/-}$ mice were also weaned onto the HFD and kept on it up to 44 wk of age (40 wk of HFD). Glucose tolerance (GTT) and insulin tolerance (ITT) tests were performed at various times (see **Figs. 1** and **2**) (33). Experimental procedures were authorized by the Cantonal Veterinary Committee (Service de la Sécurité Alimentaire et des Affaires Vétérinaires, Givisiez, Switzerland.).

Molecular measurements

Total RNA was isolated from tissues by guanidinium–thiocyanate extraction.

For quantitative real-time PCR (qPCR), cDNA was prepared with a reverse transcription kit (Promega, Madison, WI, USA), and PCR was performed with a commercial SYBR green mix (Bio-Rad, Hercules, CA, USA) and specific primers (Supplemental Table S1). Data are expressed as relative RNA levels normalized on cyclophilin. For microarray analysis, total RNAs were hybridized in quadruplicate on a whole mouse genome 4x44K microarray (G4122F; AMADID 014868; Agilent Technologies, Santa Clara, CA, USA), scanned with the Agilent microarray scanner at 5 μm resolution, and analyzed numerically with the manufacturer's software. All microarray data are available through the Gene Expression Omnibus database (National Institutes of Health, Bethesda, MD, USA; *http://www.ncbi.nlm.nih.gov/geo/*) under the accession number GSE73759. For immunoblot analysis, the antibodies were P-AKT Ser^{473}, AKT, P-FoxO1 Ser^{356}, P-FoxO1 Thr^{24}, FoxO1, catalase, and superoxide dismutase (SOD)-2 (Cell Signaling Technology, Danvers, MA, USA); HO (Enzo Life Sciences, Farmingdale, NY, USA); and Sesn2 (Proteintec, Rosemont, IL, USA). Quantification of adipose tissue crown-like structures (CLSs) was performed as described elsewhere (33). Malondialdehyde (MDA) levels were measured with a commercial kit (Abcam, Cambridge, MA, USA). Macrophage immunostaining of liver sections was performed with F4/80 antibodies (AbD Serotec, Raleigh, NC, USA). Immunofluorescence analysis of FoxO proteins in skin sections was performed with anti-Fox03a (Cell Signaling Technology) or anti-Fox04 (Abcam), and images were acquired with the Apotome microscope (Zeiss, Thornwood, NY, USA) with a ×20 objective.

Statistical analysis

Survival curves were analyzed by log-rank (Mantel-Cox) test and by Gehan-Breslow-Wilcoxon test. DNA microarray data were analyzed with the R software environment for statistical computing (*http://www.r-project.org/*) and the Bioconductor library of biostatistical packages (*http://www.bioconductor.org/*). Statistical significance was set at $P < 0.05$. The Database for Annotation, Visualization and Integrated Discovery (DAVID) resource was used for enrichment analysis of differentially expressed genes, with annotations from Gene Ontology, Kyoto Encyclopedia of Genes and Genomes (KEGG) (*http://www.genome.jp/kegg/*) and PFAM (*http://www.pfam.xfam.org*). A value of $P < 0.05$ denoted significant overrepresentation.

All other data are expressed as means ± SEM; A value of $P < 0.05$ by Student's *t* test indicates statistical significance.

RESULTS

$JNK1^{-/-}$ mice kept on an HFD display sustained protection from obesity and insulin resistance, but are predisposed to skin aging

Mice $JNK1^{-/-}$ and their WT controls were kept on an HFD after weaning, and we monitored life span, body weight, and glucose homeostasis. We did not find a statistically significant difference between the survival curves of WT and $JNK1^{-/-}$ mice, although we observed a nonsignificant tendency toward decreased age at 50% survival and increased maximum life span in $JNK1^{-/-}$ mice (Fig. 1*A*).

Body weight measurements showed that, while consuming an HFD, $JNK1^{-/-}$ mice were significantly leaner than control mice until the age of 65 wk, although by the age of 80 wk, body weight was similar between the genotypes (Fig. 1*B*). $JNK1^{-/-}$ mice at their plateau of body mass, at 50 wk of age, weighed ~13 g less than their WT control. We performed GTTs and ITTs at different time points, and we observed that $JNK1^{-/-}$ mice displayed improved insulin tolerance *vs.* control mice, at least until 48 wk of age (Fig. 1*C*). GTT on 47-wk-old mice did not reveal any difference between groups (Supplemental

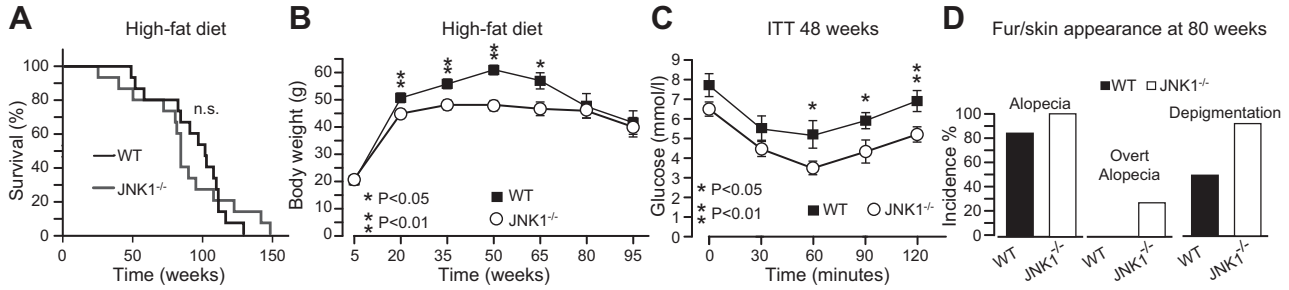

Figure 1. JNK1$^{-/-}$ mice display sustained metabolic protection from an HFD, but also display signs of exacerbated skin aging. *A*) Survival curve of 15 WT mice and 15 JNK1$^{-/-}$ mice that were kept on an HFD from weaning to death. *B*) Growth curve of the mice. *C*) ITT of 48-wk-old WT mice and JNK1$^{-/-}$ mice on an HFD. *D*) Incidence of alopecia, overt alopecia, and hair depigmentation in 80-wk-old WT mice and JNK1$^{-/-}$ mice kept on an HFD.

Fig. S1). However, comparison of GTTs performed at different time points indicated that the absence of difference between groups at 47 wk of age was due to an improvement of glucose tolerance in control mice (Supplemental Fig. S1).

During our routine health checks of the mice we observed that, compared to WT controls, JNK1$^{-/-}$ mice displayed more signs of alopecia and hair depigmentation (Fig. 1*D*).

Overall, these data indicate that JNK1 ablation leads to a long-term protection from diet-induced obesity and insulin resistance, but also indicate that JNK1 activity may protect against skin aging.

JNK1$^{-/-}$ mice display sustained protection from obesity-induced adipose tissue inflammation and insulin resistance

To reproduce the observations described above and further learn about the role of JNK1 in prolonged HFD feeding, we investigated a second independent cohort of mice, which we euthanized at 44 wk of age, when differences in fur quality between genotypes were evident. We could reproduce the sustained leaner phenotype and long-term improved insulin tolerance of JNK1$^{-/-}$ mice, although by 43 wk of age, there was no difference in glucose tolerance between genotypes (Fig. 2*A*–*H*). The latter was explained by an improved glucose tolerance of the WT mice (Fig. 2*D*, *H*), which was consistent with that observed in the previous cohort (Supplemental Fig. S1). Mac-2 immunostaining of adipose tissue sections revealed that 44-wk-old JNK1$^{-/-}$ mice, kept on an HFD, displayed a decreased number of CLSs compared to their WT controls (Fig. 2*I*, *J*). Consistently, the expression of adipose tissue macrophage markers (F4/80 and CD11c) and of cytokines associated with classic M1 macrophage activation (IL-6, TNFα, IL-1Ra, and MIP-1α) was also decreased in white adipose tissue from JNK1$^{-/-}$ mice compared to WT mice (Fig. 2*K*). Genome-wide gene expression analysis revealed that the expression of several genes implicated in immunity was down-regulated in white adipose tissues from JNK1$^{-/-}$ mice, and gene ontology analysis of these down-regulated genes indicated reduced leukocyte recruitment, and milder immune responses to chronic obesity in adipose tissues from JNK1$^{-/-}$ mice compared to that in control mice (Fig. 2*L*). Altogether, our data indicate that JNK1 ablation in mice confers long-term protection from HFD-induced adipose tissue inflammation and insulin resistance.

JNK1$^{-/-}$ mice display sustained protection from HFD-induced hepatosteatosis but not from liver inflammation

Liver histology revealed that, relative to WT mice, JNK1$^{-/-}$ mice kept on HFD were protected from hepatic steatosis at least up to 44 wk of age and 40 wk of HFD feeding (**Fig. 3*A***). However, immunostaining of liver sections with the macrophage marker F4/80 indicate that the number of liver macrophages was similar between WT and JNK1$^{-/-}$ mice (Fig. 3*B*, *C*). Consistently, qPCR analysis of liver samples indicated that F4/80 mRNA levels and expression of major proinflammatory cytokines were similar between JNK1$^{-/-}$ mice and WT control mice after long-term HFD feeding (Fig. 3*D*). Finally, genome-wide gene expression analysis of liver samples from these mice did not reveal significant differences in the expression of inflammatory genes between genotypes (data not shown). Overall, these results indicate that JNK1 ablation in mice confers sustained protection from the effects of chronic HFD feeding on hepatosteatosis, but not from liver inflammation.

JNK1$^{-/-}$ mice chronically fed an HFD are predisposed to skin damage and inflammation

JNK1$^{-/-}$ mice and WT controls kept on HFD were closely monitored for signs of alopecia and hair depigmentation. Consistent with the data from the previous cohort (Fig. 1), we observed that JNK1$^{-/-}$ mice develop alopecia and hair depigmentation before their WT controls (**Fig. 4*A*, *B***). By the age of 44 wk, both JNK1$^{-/-}$ mice and WT controls displayed at least some minor sign of alopecia (compared to young mice); however, it was more pronounced in JNK1$^{-/-}$ mice. Furthermore, we did not detect hair depigmentation in WT mice up to 44 wk of age, whereas 75% of JNK1$^{-/-}$ mice showed some depigmentation, which was quite variable within the group, ranging from minor

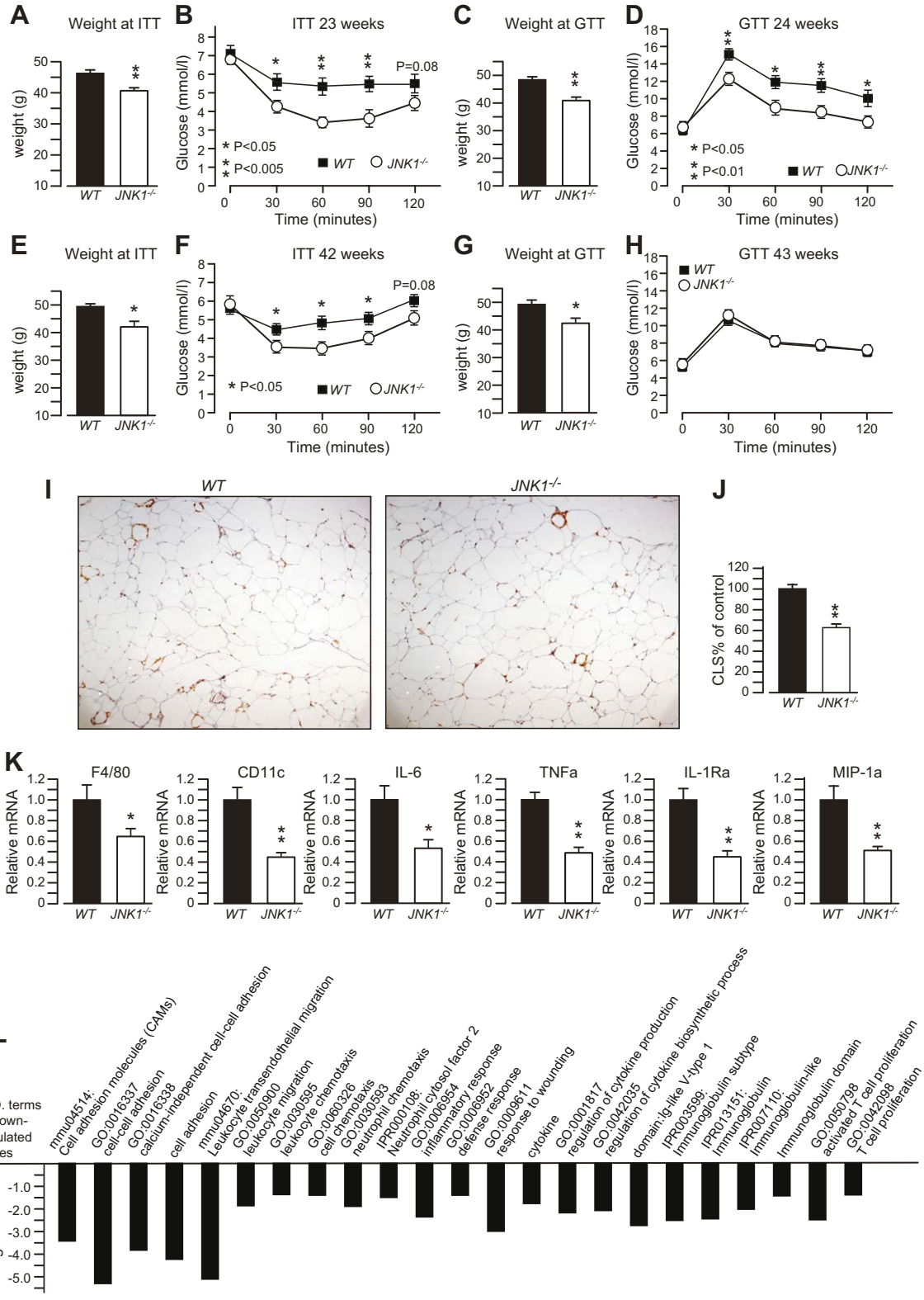

Figure 2. JNK1$^{-/-}$ mice display sustained protection against HFD-induced adipose tissue inflammation and insulin resistance. Body weight (*A*) and ITT results (*B*) of 23-wk-old WT mice and JNK1$^{-/-}$ mice kept on an HFD. Body weight (*C*) and GTT results (*D*) of 24-wk-old WT mice and JNK1$^{-/-}$ mice kept on an HFD. Body weight (*E*) and ITT results (*F*) of the same mice at the age of 42 wk. Body weight (*G*) and GTT results (*H*) of the same mice at the age of 43 wk. *I*) Mac2 staining of CLSs of adipose tissue sections from the mice at the age of 44 wk. *J*) Quantification of the number of CLSs from (*I*). *K*) Real-time qPCR analysis of the expression of proinflammatory genes in adipose tissue of the mice in (*I*). *L*) Significant terms from a gene ontology analysis of DNA microarray data, for genes that were down-regulated in adipose tissue of the JNK1$^{-/-}$ mice *vs.* their controls.

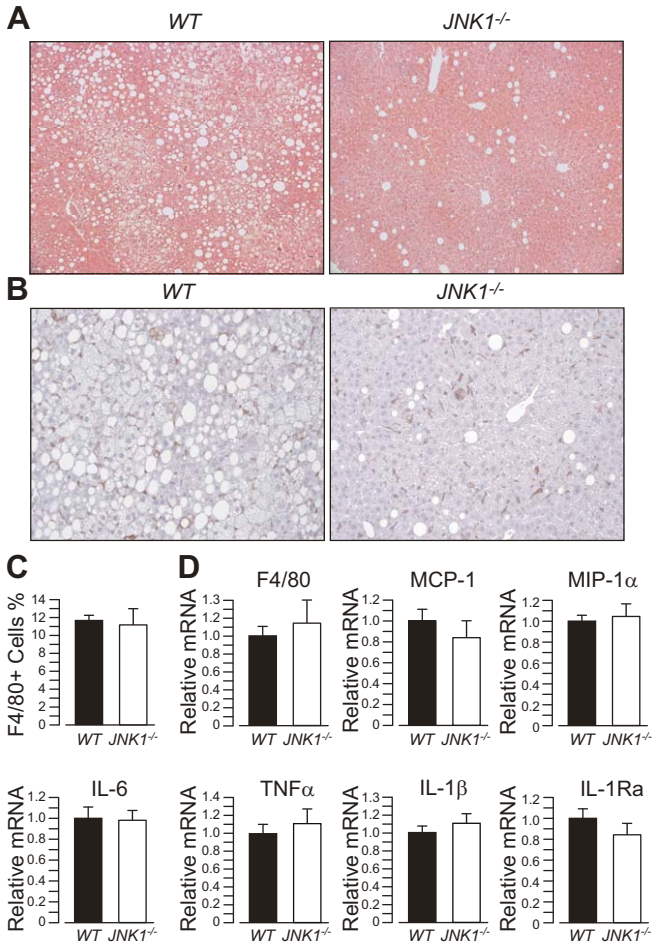

Figure 3. JNK1$^{-/-}$ mice display sustained protection against HFD-induced steatosis, but not against liver inflammation. *A*) Hematoxylin and eosin staining of representative liver sections of 44-wk-old WT mice and JNK1$^{-/-}$ mice kept on an HFD. *B*) F4/80 immunostaining of liver sections from the same mice. *C*) Quantification of the number of F4/80^{+} cells from the liver sections in (*B*). *D*) Real-time qPCR analysis of the expression of proinflammatory genes in mouse liver.

depigmentation to overt (**Fig. 4*A, B***). Histologic analysis of skin samples showed that epidermal thickness was significantly increased in JNK1$^{-/-}$ mice, which also displayed signs of inflammation (Fig. 4*C*, *D*). qPCR analysis revealed an induction of the expression of genes associated with M1 macrophage activation (IL-6, -1β, and -1Ra) and decreased expression of genes associated with alternative M2 macrophage activation (MGL-1, MRC-2, and FIZZ1) (Fig. 4*E*). These data indicate that skin macrophages of JNK1$^{-/-}$ mice are polarized toward an M1 proinflammatory phenotype, which is consistent with the skin histology data, and in marked contrast with what was observed in adipose tissue. To further learn about the pathways altered in the skin of JNK1$^{-/-}$ mice, we performed genome-wide gene expression analysis of skin samples and analyzed the data by gene ontology analysis. The results revealed that several genes related to keratinization, epidermis development, hair cycle, pigmentation, and inflammation were up-regulated in skin samples from JNK1$^{-/-}$ mice compared with gene expression in samples from WT controls (Fig. 4*F*). This pattern of gene expression is consistent with the idea of increased tissue damage, inflammation, and repair in the skin of JNK1$^{-/-}$ mice.

Taken together, our data indicate that JNK1$^{-/-}$ mice kept on an HFD for a prolonged period are predisposed to skin damage and inflammation.

JNK1 ablation has opposite effects on fat and skin oxidative damage in mice fed an HFD for a prolonged period

To evaluate the effects of JNK1 ablation on oxidative stress damage in mice kept on an HFD, we measured the levels of the lipid peroxidation product MDA in different tissues from the WT mice and JNK1$^{-/-}$ mice described above.

MDA levels were similar between genotypes in kidney and heart, were slightly but significantly decreased in liver, and were markedly decreased in white adipose tissue from JNK1$^{-/-}$ mice compared with levels in WT controls (**Fig. 5*A***). By contrast, MDA levels were significantly elevated in skin samples from JNK1$^{-/-}$ mice compared to WT controls indicating increased oxidative damage in this tissue. To further learn about the mechanisms of increased oxidative damage in the skin of JNK1$^{-/-}$ mice, we measured mRNA levels of HO-1, a potent antioxidant and anti-inflammatory enzyme with expression that has been shown to be elevated in keratinocyte cell cultures by oxidative stress inducers and by lipid peroxidation products in a JNK1-dependent manner (34, 35). HO-1 mRNA levels were similar between genotypes in kidney, heart, and liver, but were markedly reduced in white adipose tissue of JNK1$^{-/-}$ mice compared to WT controls (Fig. 5*B*). This pattern of gene expression parallels the MDA levels in these tissues and is consistent with the concept of HO-1 as an oxidative stress and lipid-peroxidation–responsive gene. However, we also observed that HO-1 mRNA levels were significantly lower in the skin of JNK1$^{-/-}$ mice *vs*. WT controls, despite increased MDA levels in the former. This observation is consistent with keratinocyte cell culture studies indicating a major role for JNK1 in the induction of HO-1 gene expression in response to oxidative stress and lipid peroxidation products. We then used real-time qPCR to measure the expression of several genes implicated in oxidative stress tolerance in skin samples from WT mice and JNK1$^{-/-}$ mice.

The results show that mRNA levels of Sesn-2 and catalase were also significantly decreased in skin samples from JNK1$^{-/-}$ mice (Fig. 5C). These differences may explain the increased oxidative damage in the skin of JNK1$^{-/-}$ mice, despite the systemic metabolic protection and decreased oxidative damage in fat and liver. Catalase, in particular, has been shown to play a major role in skin and hair tolerance to oxidative stress (36, 37). Immunoblot analysis indicated that HO-1 and Sesn-2 protein levels were only marginally reduced in JNK1$^{-/-}$ mice, and the differences were not statistically significant. However, catalase and SOD2 protein levels were markedly reduced in skin samples from JNK1$^{-/-}$ mice. mRNA levels of catalase, Sesn-2, and SOD-2 were not reduced in adipose

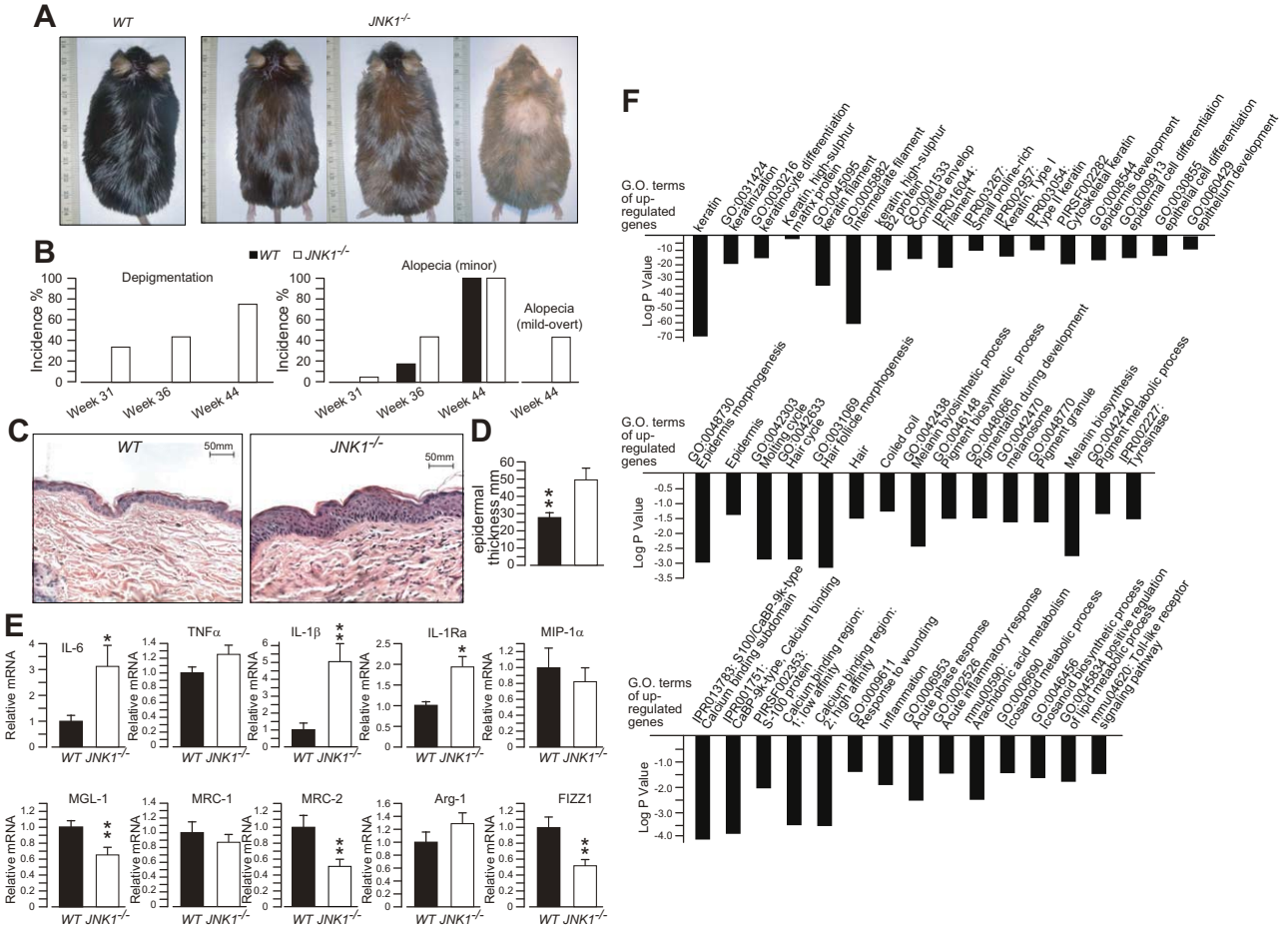

Figure 4. JNK1$^{-/-}$ mice fed an HFD for a prolonged period are predisposed to skin damage and inflammation. *A*) Representative photographs of 44-wk-old WT and JNK1$^{-/-}$ mice kept on an HFD. *B*) Incidence of hair depigmentation, alopecia (any sign), and mild-to-overt alopecia in the same mice. *C*) Hematoxylin and eosin staining of representative skin sections of the mice. *D*) Average epidermal thickness of 44-wk-old WT and JNK1$^{-/-}$ mice kept on an HFD. *E*) Real-time qPCR analysis of the expression of M1 cytokines (top) and M2 genes (bottom) in skin samples of WT and JNK1$^{-/-}$ mice. *F*) Significant terms from a gene ontology analysis of DNA microarray data for genes with expression induced in the skin of JNK1$^{-/-}$ mice compared to WT controls.

tissue, liver, heart, and kidney samples from JNK1$^{-/-}$ mice *vs.* their controls (Supplemental Fig. S2). Because catalase and SOD2 expression are controlled by FoxO transcription factors, we evaluated the activation of FoxOs proteins and of their regulator AKT in the skin of the mice. Our data showed that AKT activation and FoxO1 phosphorylation by AKT were similar in the skin of WT and JNK1$^{-/-}$ mice (Supplemental Fig. S3*A*, *B*). Furthermore, immunostaining of skin sections with FoxO3a- and FoxO4-specific antibodies revealed an almost complete nuclear localization of FoxO3a and FoxO4 in the skins of both genotypes (Supplemental Fig. S3*C*).

Altogether, our results indicate that systemic JNK1 ablation leads to decreased oxidative damage in liver and white adipose tissue and, by contrast, increased skin oxidative damage and reduced expression antioxidant genes specifically in the skin.

DISCUSSION

Several studies have demonstrated that JNK1 ablation protects mice from diet-induced obesity and insulin resistance (8–11, 16, 17). However, these medium-term studies do not exceed 20 wk of dietary treatment, and thus the long-term effects of JNK1 inhibition in obesity are largely unknown. In this study, we investigated for the first time the late effects of JNK1 inactivation in aging mice exposed for a prolonged period to an obesogenic HFD. Our JNK1$^{-/-}$ mice kept on an HFD were mildly predisposed to skin oxidative damage and inflammation. However, the metabolic protection from the effects of dietary fat caused by JNK1 ablation was largely sustained over least 40 wk of an HFD, and this improved metabolism was paralleled by reduced oxidative damage in liver and adipose tissue. The protection from oxidative damage observed in liver and fat of JNK1$^{-/-}$ mice can thus be explained by decreased adiposity and reduced adipose tissue inflammation observed in the mice, which is believed to have major local and systemic effects (17). In line with this interpretation, MDA levels were significantly but modestly reduced in liver and markedly reduced in white adipose tissue of JNK1$^{-/-}$ mice *vs.* their WT controls. Furthermore, we observed that, although the JNK1$^{-/-}$ mice displayed long-term protection from fatty liver, hepatic inflammation in them was similar to that in WT

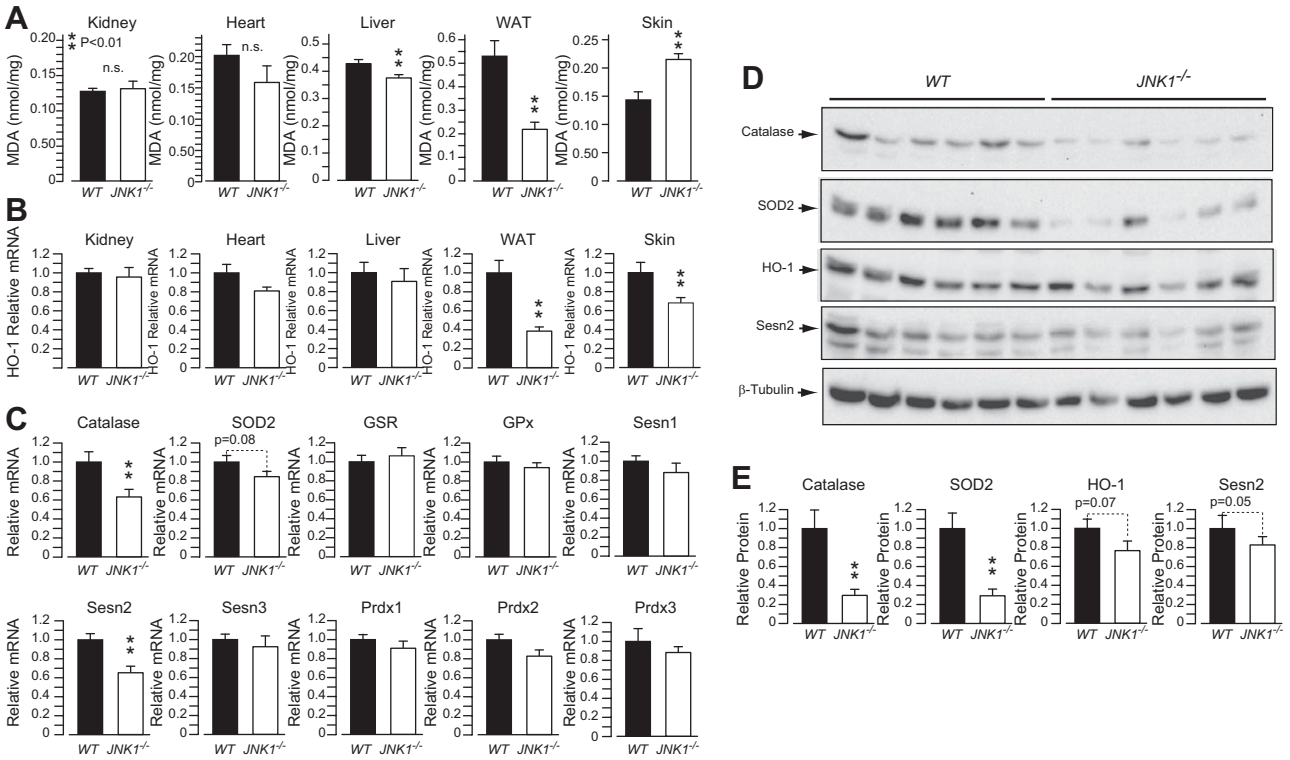

Figure 5. Loss of JNK1 in mice fed an HFD for a prolonged period protects liver and adipose tissue, but predisposes skin to oxidative damage. *A*) MDA levels in different tissues from 44-wk-old WT and JNK1$^{-/-}$ kept on an HFD. *B*) Real-time qPCR analysis of the expression of HO-1 in the tissues. *C*) qPCR analysis of the expression of genes implicated in oxidative stress tolerance in the skin of the same mice. *D*) Immunoblot analysis of catalase, SOD2, HO-1, and Sesn-2 protein levels in the skin samples in (*C*). *E*) Quantification of the immunoblots panel *D*. WAT, white adipose tissue.

controls after 40 wk of an HFD, indicating limited protection in this tissue and a more specific role for JNK1 in the control of adipose tissue inflammation. It is possible that the lack of long-term protection from liver inflammation observed in the JNK1$^{-/-}$ mice is the result of a compensatory action from JNK2. Indeed, targeted deletion of JNK1 in liver has been reported to cause hepatic microsteatosis, whereas compound deletion of JNK1 and -2 was protective (38, 39). This observation suggests that simultaneous targeting of JNK1 and -2 may be a more effective antidiabetogenic strategy than targeting JNK1 in isolation. However, that mouse embryonic fibroblasts lacking JNK1 and -2 are more sensitive to hydrogen peroxide is a possible concern (32). Indeed, our observation that JNK1$^{-/-}$ mice fed an HFD over a long period displayed increased skin oxidative damage and reduced antioxidant gene expression implies a role for JNK1 in promoting oxidative stress tolerance in this tissue.

A limitation of our study is that only male mice were investigated; thus, the impact of female steroids on the observed phenotype remains unresolved. Another major limitation of our study is that the use of systemic JNK1 inactivation does not allow the identification of the specific cell type implicated in the increased skin oxidative damage observed in JNK1$^{-/-}$ mice. Therefore, our data do not exclude a non–cell-autonomous action of JNK1 in promoting oxidative stress tolerance. Nonetheless, a role for JNK in the control of antioxidant gene expression in cultured skin cells has been reported (34, 35, 40, 41), and that the skin was the only tissue of JNK1$^{-/-}$ mice displaying increased oxidative damage is consistent with the idea that JNK1 activity within a specific skin cell type may protect against local oxidative damage. Indeed, because JNK1 deletion improves metabolic homeostasis and reduces adiposity, the expected systemic outcome of JNK1 deletion would be reduced oxidative stress, as observed in liver and adipose tissue. We found that mice lacking JNK1 and having prolonged exposure to an HFD displayed, specifically in skin cells, reduced mRNA and protein levels of catalase, an enzyme playing a major role in skin tolerance to oxidative stress, whose reduced expression correlates strongly with hair depigmentation (36, 37). Furthermore, we observed a marked reduction of SOD2 protein levels and decreased mRNA levels of the antioxidant genes Sesn-2 and HO-1 in the skin of JNK1 mice. Because catalase and SOD2 expression is controlled by FoxO transcription factors, it is possible that the effects of JNK1 activity on skin catalase levels are mediated by JNK1s effect on FoxOs proteins (27). However, other mechanisms may also be involved, as we did not observe signs of reduced FoxO1 activation and of FoxO3a and -O4 nuclear localization in skin samples from JNK1$^{-/-}$ mice. Furthermore, SOD2, HO-1, and Sesn-2 have been reported to be directly regulated by the JNK-AP1 pathway in a cell-autonomous fashion (28–31, 40). Hence, the increased oxidative damage in the skin of JNK1$^{-/-}$ mice could be

explained by a local effect on antioxidant gene expression. We observed some discrepancies between mRNAs and protein levels of the antioxidant genes with downregulated expression in the skin of JNK1$^{-/-}$ mice. Sesn2 and HO-1 mRNA levels were significantly reduced in the skin of JNK1$^{-/-}$ mice, whereas we observed only a marginal, statistically nonsignificant, reduction in SOD2 mRNA levels. By contrast, SOD2 protein content was markedly reduced in the skin of JNK1$^{-/-}$ mice, whereas HO-1 and Sesn2 protein levels were only marginally reduced, and these differences did not reach statistical significance. Only catalase was consistently reduced at the mRNA and protein levels, although the observed differences in protein levels were larger than for the differences in mRNA content. The reasons for these apparent discrepancies are not clear and may suggest posttranscriptional regulation mechanisms. However, it should be considered that these genes are rhythmically expressed in a circadian fashion (42), and the observed differences in mRNA and protein content may be caused by a lag time between the circadian changes in mRNA and protein levels consequent to the relative abundance and stability of these proteins.

Overall, our data show that the effects of JNK1 ablation on oxidative stress tolerance in obese mice are specific for the skin and are less dramatic than those reported in the *Drosophila* and *Caenorhabditis elegans* models (23–26). Furthermore, we show that protection against obesity, adipose tissue inflammation, steatosis, and insulin resistance is largely sustained over a long period in JNK1$^{-/-}$ and is paralleled by reduced oxidative damage in white adipose tissue and liver. Our results suggest that prolonged use of drugs targeting JNK may predispose patients to skin oxidative damage; however, this possible side effect can be easily detected and may be largely preventable by minimizing skin exposure to oxidative stress sources such as irritants and UV radiation. Indeed, JNK is a UV-responsive kinase (43) that is activated in human skin by UV light (44).

We conclude that JNK1 should be regarded as an effective and relatively safe target for long-term treatment of obesity and insulin resistance and that compounds that target JNK1 in brain and adipose tissue and do not accumulate in the skin could be the more effective and safer drug candidates. FJ

This work was supported by grants from the Swiss National Science Foundation, the Swedish Diabetes Foundation, the Swedish Research Council, and a startup package from the University of Gothenburg (to G.S.). Author contributions: B. Becattini and F. Zani performed most of the experiments, analyzed data, and contributed to the discussion; L. Breasson and C. Sardi performed experiments; V. G. D'Agostino and A. Provenzani performed the DNA microarray analysis; M.-K. Choo and J. M. Park performed the skin histopathological analysis and discussed the skin data; G. Solinas conceived the project, the experimental design, and wrote the manuscript; B. Becattini, F. Zani, A. Provenzani, M.-K. Choo and J. M. Park, significantly contributed to the writing of the manuscript with their comments; and all authors approved the paper. The authors declare no conflicts of interest.

REFERENCES

1. Solinas, G. (2012) Molecular pathways linking metabolic inflammation and thermogenesis. *Obes. Rev.* **13**(Suppl 2), 69–82
2. Solinas, G., and Karin, M. (2010) JNK1 and IKKbeta: molecular links between obesity and metabolic dysfunction. *FASEB J.* **24**, 2596–2611
3. Virtue, S., and Vidal-Puig, A. (2008) It's not how fat you are, it's what you do with it that counts. *PLoS Biol.* **6**, e237
4. Unger, R. H., Clark, G. O., Scherer, P. E., and Orci, L. (2010) Lipid homeostasis, lipotoxicity and the metabolic syndrome. *Biochim. Biophys. Acta* **1801**, 209–214
5. Hotamisligil, G. S. (2006) Inflammation and metabolic disorders. *Nature* **444**, 860–867
6. Donath, M.Y. (2014) Targeting inflammation in the treatment of type 2 diabetes: time to start. *Nat. Rev. Drug Discov.* **13**, 465–476
7. Aguirre, V., Uchida, T., Yenush, L., Davis, R., and White, M. F. (2000) The c-Jun NH(2)-terminal kinase promotes insulin resistance during association with insulin receptor substrate-1 and phosphorylation of Ser(307). *J. Biol. Chem.* **275**, 9047–9054
8. Hirosumi, J., Tuncman, G., Chang, L., Görgün, C. Z., Uysal, K. T., Maeda, K., Karin, M., and Hotamisligil, G. S. (2002) A central role for JNK in obesity and insulin resistance. *Nature* **420**, 333–336
9. Tuncman, G., Hirosumi, J., Solinas, G., Chang, L., Karin, M., and Hotamisligil, G. S. (2006) Functional in vivo interactions between JNK1 and JNK2 isoforms in obesity and insulin resistance. *Proc. Natl. Acad. Sci. USA* **103**, 10741–10746
10. Solinas, G., Naugler, W., Galimi, F., Lee, M. S., and Karin, M. (2006) Saturated fatty acids inhibit induction of insulin gene transcription by JNK-mediated phosphorylation of insulin-receptor substrates. *Proc. Natl. Acad. Sci. USA* **103**, 16454–16459
11. Solinas, G., Vilcu, C., Neels, J. G., Bandyopadhyay, G. K., Luo, J. L., Naugler, W., Grivennikov, S., Wynshaw-Boris, A., Scadeng, M., Olefsky, J. M., and Karin, M. (2007) JNK1 in hematopoietically derived cells contributes to diet-induced inflammation and insulin resistance without affecting obesity. *Cell Metab.* **6**, 386–397
12. Aguirre, V., Werner, E. D., Giraud, J., Lee, Y. H., Shoelson, S. E., and White, M. F. (2002) Phosphorylation of Ser307 in insulin receptor substrate-1 blocks interactions with the insulin receptor and inhibits insulin action. *J. Biol. Chem.* **277**, 1531–1537
13. Sabio, G., Cavanagh-Kyros, J., Barrett, T., Jung, D. Y., Ko, H. J., Ong, H., Morel, C., Mora, A., Reilly, J., Kim, J. K., and Davis, R. J. (2010) Role of the hypothalamic-pituitary-thyroid axis in metabolic regulation by JNK1. *Genes Dev.* **24**, 256–264
14. Tsaousidou, E., Paeger, L., Belgardt, B. F., Pal, M., Wunderlich, C. M., Brönneke, H., Collienne, U., Hampel, B., Wunderlich, F. T., Schmidt-Supprian, M., Kloppenburg, P., and Brüning, J. C. (2014) Distinct roles for JNK and IKK activation in Agouti-related peptide Neurons in the development of obesity and insulin resistance. *Cell Reports* **9**, 1495–1506
15. Belgardt, B. F., Mauer, J., Wunderlich, F. T., Ernst, M. B., Pal, M., Spohn, G., Brönneke, H. S., Brodesser, S., Hampel, B., Schauss, A. C., and Brüning, J. C. (2010) Hypothalamic and pituitary c-Jun N-terminal kinase 1 signaling coordinately regulates glucose metabolism. *Proc. Natl. Acad. Sci. USA* **107**, 6028–6033
16. Han, M. S., Jung, D. Y., Morel, C., Lakhani, S. A., Kim, J. K., Flavell, R. A., and Davis, R. J. (2013) JNK expression by macrophages promotes obesity-induced insulin resistance and inflammation. *Science* **339**, 218–222
17. Perry, R. J., Camporez, J. P., Kursawe, R., Titchenell, P. M., Zhang, D., Perry, C. J., Jurczak, M. J., Abudukadier, A., Han, M. S., Zhang, X. M., Ruan, H. B., Yang, X., Caprio, S., Kaech, S. M., Sul, H. S., Birnbaum, M. J., Davis, R. J., Cline, G. W., Petersen, K. F., and Shulman, G. I. (2015) Hepatic acetyl CoA links adipose tissue inflammation to hepatic insulin resistance and type 2 diabetes. *Cell* **160**, 745–758
18. Furukawa, S., Fujita, T., Shimabukuro, M., Iwaki, M., Yamada, Y., Nakajima, Y., Nakayama, O., Makishima, M., Matsuda, M., and Shimomura, I. (2004) Increased oxidative stress in obesity and its impact on metabolic syndrome. *J. Clin. Invest.* **114**, 1752–1761
19. Urakawa, H., Katsuki, A., Sumida, Y., Gabazza, E. C., Murashima, S., Morioka, K., Maruyama, N., Kitagawa, N., Tanaka, T., Hori, Y., Nakatani, K., Yano, Y., and Adachi, Y. (2003) Oxidative stress is associated with adiposity and insulin resistance in men. *J. Clin. Endocrinol. Metab.* **88**, 4673–4676
20. Shaukat, Z., Liu, D., Hussain, R., Khan, M., and Gregory, S. L. (2016) The role of JNK signalling in responses to oxidative DNA damage. *Curr. Drug Targets* 17, 154–163

21. Wagner, E. F., and Nebreda, A. R. (2009) Signal integration by JNK and p38 MAPK pathways in cancer development. *Nat. Rev. Cancer* **9**, 537–549
22. Luo, J. L., Kamata, H., and Karin, M. (2005) IKK/NF-kappaB signaling: balancing life and death: a new approach to cancer therapy. *J. Clin. Invest.* **115**, 2625–2632
23. Oh, S. W., Mukhopadhyay, A., Svrzikapa, N., Jiang, F., Davis, R. J., and Tissenbaum, H. A. (2005) JNK regulates lifespan in Caenorhabditis elegans by modulating nuclear translocation of forkhead transcription factor/DAF-16. *Proc. Natl. Acad. Sci. USA* **102**, 4494–4499
24. Wang, M. C., Bohmann, D., and Jasper, H. (2005) JNK extends life span and limits growth by antagonizing cellular and organism-wide responses to insulin signaling. *Cell* **121**, 115–125
25. Wang, M. C., Bohmann, D., and Jasper, H. (2003) JNK signaling confers tolerance to oxidative stress and extends lifespan in Drosophila. *Dev. Cell* **5**, 811–816
26. Uno, M., Honjoh, S., Matsuda, M., Hoshikawa, H., Kishimoto, S., Yamamoto, T., Ebisuya, M., Yamamoto, T., Matsumoto, K., and Nishida, E. (2013) A fasting-responsive signaling pathway that extends life span in C. elegans. *Cell Reports* **3**, 79–91
27. Eijkelenboom, A., and Burgering, B. M. (2013) FOXOs: signalling integrators for homeostasis maintenance. *Nat. Rev. Mol. Cell Biol.* **14**, 83–97
28. Lee, J. H., Budanov, A. V., and Karin, M. (2013) Sestrins orchestrate cellular metabolism to attenuate aging. *Cell Metab.* **18**, 792–801
29. Zhang, X. Y., Wu, X. Q., Deng, R., Sun, T., Feng, G. K., and Zhu, X. F. (2013) Upregulation of sestrin 2 expression via JNK pathway activation contributes to autophagy induction in cancer cells. *Cell. Signal.* **25**, 150–158
30. Yi, L., Li, F., Yong, Y., Jianting, D., Liting, Z., Xuansheng, H., Fei, L., and Jiewen, L. (2014) Upregulation of sestrin-2 expression protects against endothelial toxicity of angiotensin II. *Cell Biol. Toxicol.* **30**, 147–156
31. Kietzmann, T., Samoylenko, A., and Immenschuh, S. (2003) Transcriptional regulation of heme oxygenase-1 gene expression by MAP kinases of the JNK and p38 pathways in primary cultures of rat hepatocytes. *J. Biol. Chem.* **278**, 17927–17936
32. Ventura, J. J., Cogswell, P., Flavell, R. A., Baldwin, A. S., Jr., and Davis, R. J. (2004) JNK potentiates TNF-stimulated necrosis by increasing the production of cytotoxic reactive oxygen species. *Genes Dev.* **18**, 2905–2915
33. Becattini, B., Marone, R., Zani, F., Arsenijevic, D., Seydoux, J., Montani, J. P., Dulloo, A. G., Thorens, B., Preitner, F., Wymann, M. P., and Solinas, G. (2011) PI3Kγ within a nonhematopoietic cell type negatively regulates diet-induced thermogenesis and promotes obesity and insulin resistance. *Proc. Natl. Acad. Sci. USA* **108**, E854–E863
34. Ray, P. D., Huang, B. W., and Tsuji, Y. (2015) Coordinated regulation of Nrf2 and histone H3 serine 10 phosphorylation in arsenite-activated transcription of the human heme oxygenase-1 gene. *Biochim. Biophys. Acta* **1849**, 1277–1288
35. Zheng, R., Heck, D. E., Mishin, V., Black, A. T., Shakarjian, M. P., Kong, A. N., Laskin, D. L., and Laskin, J. D. (2014) Modulation of keratinocyte expression of antioxidants by 4-hydroxynonenal, a lipid peroxidation end product. *Toxicol. Appl. Pharmacol.* **275**, 113–121
36. Kauser, S., Westgate, G. E., Green, M. R., and Tobin, D. J. (2011) Human hair follicle and epidermal melanocytes exhibit striking differences in their aging profile which involves catalase. *J. Invest. Dermatol.* **131**, 979–982
37. Maresca, V., Flori, E., Briganti, S., Mastrofrancesco, A., Fabbri, C., Mileo, A. M., Paggi, M. G., and Picardo, M. (2008) Correlation between melanogenic and catalase activity in in vitro human melanocytes: a synergic strategy against oxidative stress. *Pigment Cell Melanoma Res.* **21**, 200–205
38. Vernia, S., Cavanagh-Kyros, J., Barrett, T., Tournier, C., and Davis, R. J. (2016) Fibroblast growth factor 21 mediates glycemic regulation by hepatic JNK. *Cell Rep.* **14**, 2273–2280
39. Sabio, G., Cavanagh-Kyros, J., Ko, H. J., Jung, D. Y., Gray, S., Jun, J. Y., Barrett, T., Mora, A., Kim, J. K., and Davis, R. J. (2009) Prevention of steatosis by hepatic JNK1. *Cell Metab.* **10**, 491–498
40. Son, Y. O., Hitron, J. A., Cheng, S., Budhraja, A., Zhang, Z., Lan Guo, N., Lee, J. C., and Shi, X. (2011) The dual roles of c-Jun NH2-terminal kinase signaling in Cr(VI)-induced apoptosis in JB6 cells. *Toxicol. Sci.* **119**, 335–345
41. Zheng, R., Heck, D. E., Black, A. T., Gow, A., Laskin, D. L., and Laskin, J. D. (2014) Regulation of keratinocyte expression of stress proteins and antioxidants by the electrophilic nitrofatty acids 9- and 10-nitrooleic acid. *Free Radic. Biol. Med.* **67**, 1–9
42. Patel, S. A., Velingkaar, N. S., and Kondratov, R. V. (2014) Transcriptional control of antioxidant defense by the circadian clock. *Antioxid. Redox Signal.* **20**, 2997–3006
43. Hibi, M., Lin, A., Smeal, T., Minden, A., and Karin, M. (1993) Identification of an oncoprotein- and UV-responsive protein kinase that binds and potentiates the c-Jun activation domain. *Genes Dev.* **7**, 2135–2148
44. Fisher, G. J., Talwar, H. S., Lin, J., Lin, P., McPhillips, F., Wang, Z., Li, X., Wan, Y., Kang, S., and Voorhees, J. J. (1998) Retinoic acid inhibits induction of c-Jun protein by ultraviolet radiation that occurs subsequent to activation of mitogen-activated protein kinase pathways in human skin in vivo. *J. Clin. Invest.* **101**, 1432–1440

S1

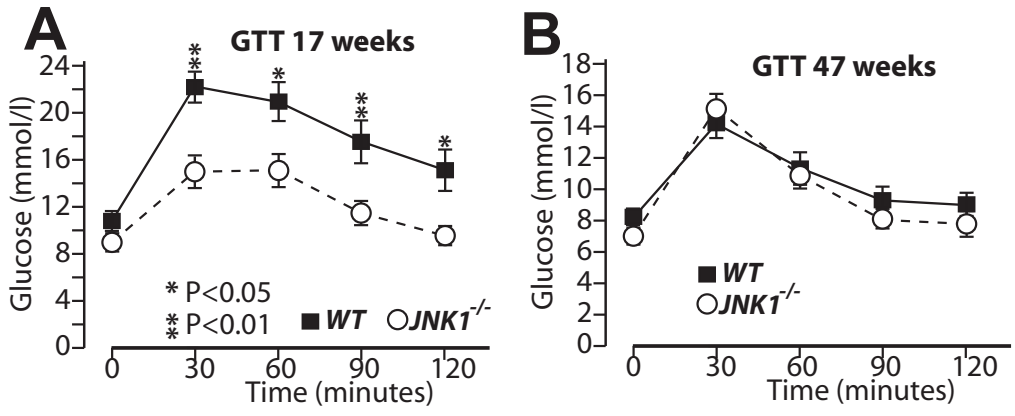

Figure S1. Glucose tolerance in WT and JNK1-/- mice on chronic high-fat diet. Glucose tolerance tests (GTT) of the mice described in figure 1.
15 WT and 15 JNK1-/- mice were kept on HFD from weaning and GTT was performed via intraperitoneal injection of 1g for glucose per Kg of body weight at the age of 17 weeks (A), and of 47 weeks (B).

S2

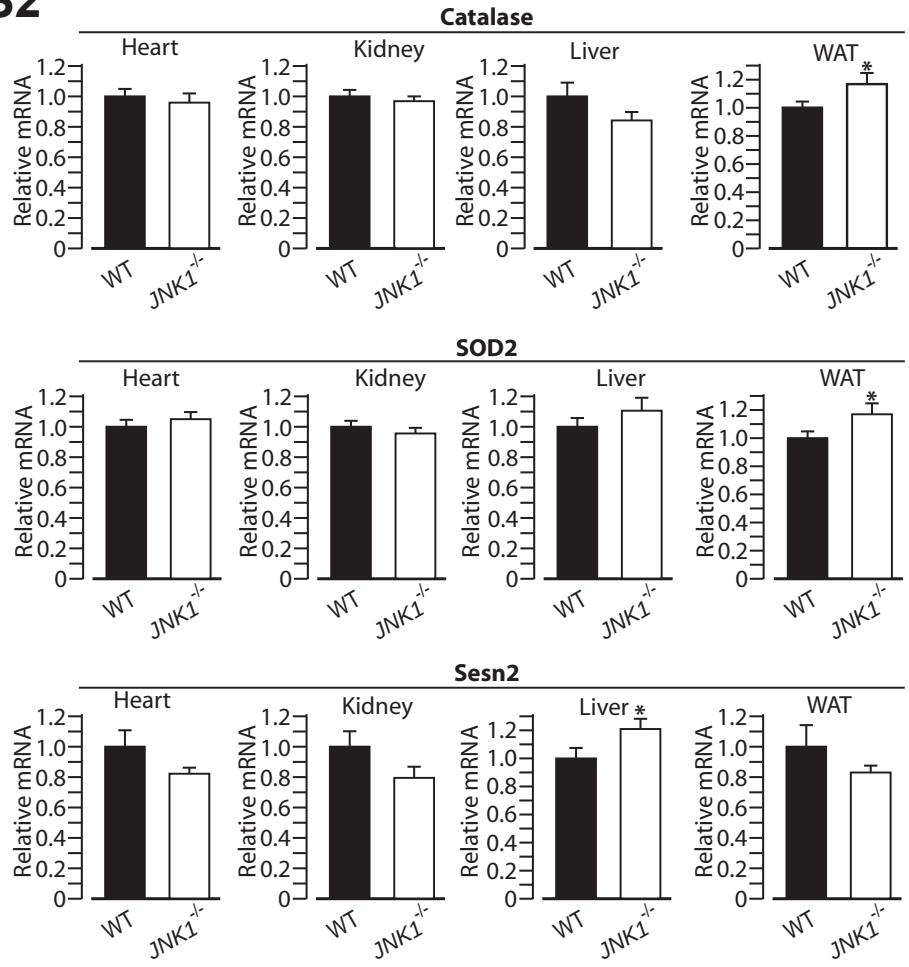

Figure S2. Expression of antioxidant genes in metabolically relevant tissues. The expression of the FOXOs target genes catalase and SOD2 and the AP1 target gene Sesn2 was measured by qPCR in heart, kidney, liver and adipose tissue.

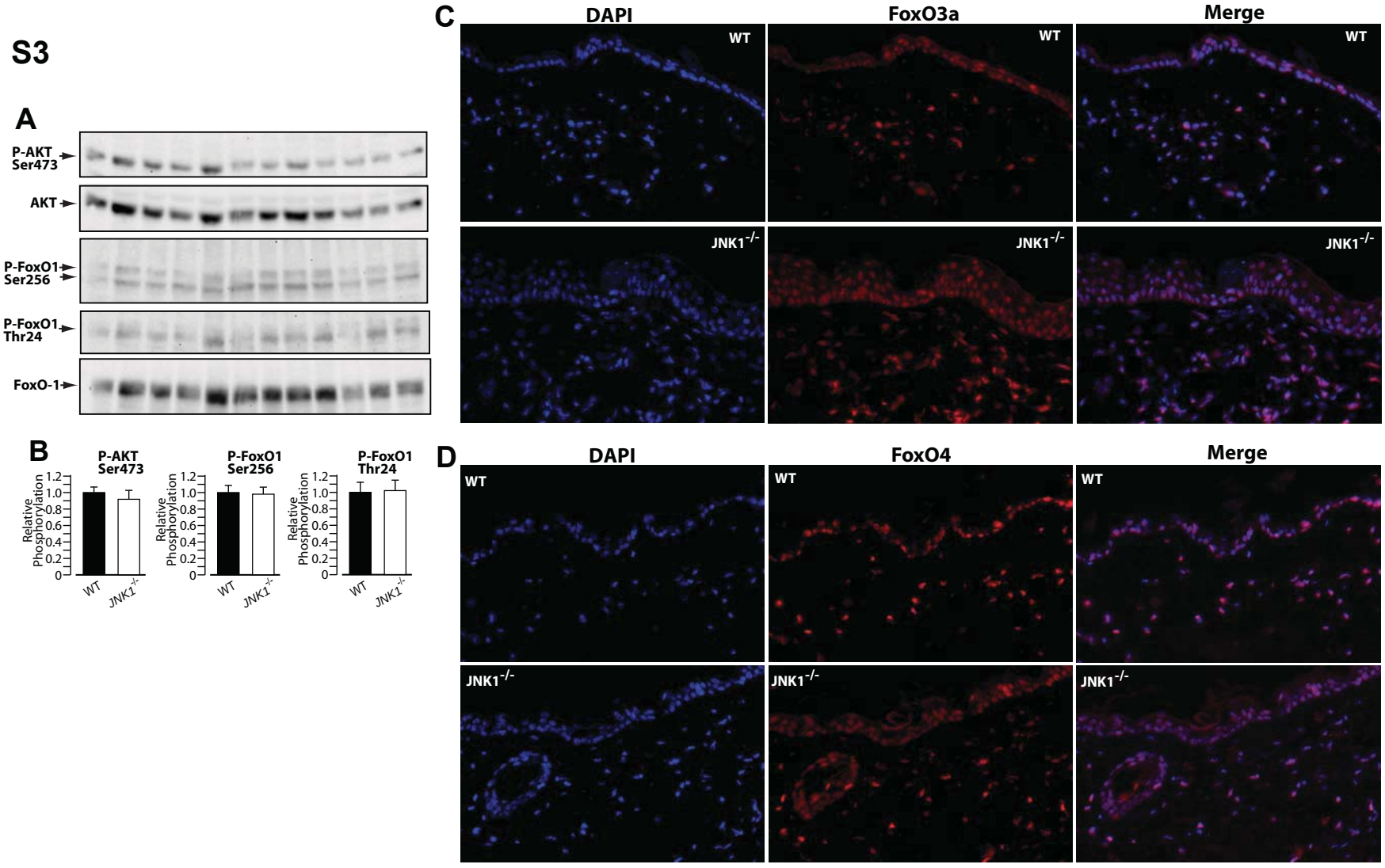

Figure S3. (A) Immunoblot analysis of AKT phosphorylation, and FoxO1 phosphorylation at its AKT phosphorylation sites of the skin samples described in figure 4C. (B) Quantification of the blots in A. (C) FoxO3a Immunoflurescence staining of the skin sections above. (D) FoxO4 Immunoflurescence staining of the skin sections above.

Supplemental Table S1. List of primers used in qPCR reactions

Name	Forward	Reverse
Cyclo	ATG GTC AAC CCC ACC GTG T	TTT CTG CTG TCT TTG GAA CTT TGT C
F4/80	CTT TGG CTA TGG GCT TCC AGT C	GCA AGG AGG ACA GAG TTT ATC GTG
CD11c (Itgax)	CTG GAT AGC CTT TCT TCT GCT G	GCA CAC TGT GTC CGA ACT C
IL-1β	GCA ACT GTT CCT GAA CTC AAC T	TCT TTT GGG GTC CGT CAA CT
TNF-a	CCC CAA AGG GAT GAG AAG TT	CTC CTC CAC TTG GTG GTT TG
MIP-1a	TTC TCT GTA CCA TGA CAC TCT GC	CGT GGA ATC TTC CGG CTG TAG
MCP-1	CCC CAA GAA GGA ATG GGT CC	GGT TGT GGA AAA GGT AGT GG
IL-6	TCC TAC CCC AAT TTC CAA TGC TC	TTG GAT GGT CTT GGT CCT TAG CC
IL-1Rn	AAA TCT GCT GGG GAC CCT AC	TCT TCT AGT TTG ATA TTT GGT CCT TG
GSR	GGG TGG CAC TTG CGT GAA TG	TTC AGG CGG CTC ACA TAG GC
GPx	GTG AGC CTG GGC TCC CTG CG	ACT TGA GGG AAT TCA GAA TC
CAT	TCA GGA TGT GGT TTT CAC TG	GTG TAA AAT TTC ACT GCA AAC
SOD2	TCA TGC AGC TGC ACC ACA GC	CCA TTG AAC TTC AGT GCA GG
UCP2	ATG GTT GGT TTC AAG GCC ACA	TTG GCG GTA TCC AGA GGG AA
Sesn1	CGG ACC AAG CAG GTT CAT CC	TGA TGT TAT CCA GAC GAC CCA AA
Sesn2	TAG CCT GCA GCC TCA CCT AT	TAT CTG ATG CCA AAG ACG CA
Sesn3	CAT GCG TTT CCT CAC TCA GA	GGC AAA GTC TTC GTA CCC AA
PRDX1	AAT GCA AAA ATT GGG TAT CCT GC	CGT GGG ACA CAC AAA AGT AAA GT
PRDX2	CAC CTG GCG TGG ATC AAT ACC	GAC CCC TGT AAG CAA TGC CC
PRDX3	TTAGCACCAGTTCCTCTTTCCA	CCCTTAAAGTCGTCGAGACTCA
HO-1	GGT GAT GGC TTC CTT GTA CC	AGT GAG GCC CAT ACC AGA AG